Peristaltic Contrast Media Injection Improved Image Quality and Decreased Radiation and Contrast Dose When Compared With Direct Drive Injection During Liver Computed Tomography

Charbel Saade, PhD, Lina Karout, MD,† Sarah Khalife, BSc,* Ahmad Mayat, FRANZCR,‡ Sugendran Pillay, FRANZCR,§ Edward Chan, MBBS, MPhil,§ Gilbert Maroun, MD,† Raquelle Alam, MD,† Mohammad Abu Shattal, MD,† and Lena Naffaa, MD†*

Purpose: The aim of this study was to compare hepatic vascular and parenchymal image quality between direct and peristaltic contrast injectors during hepatic computed tomography (HCT).

Methods: Patients (n = 171) who underwent enhanced HCT and had both contrast media protocols and injector systems were included; group A: direct-drive injector with fixed 100 mL contrast volume (CV), and group B: peristaltic injector with weight-based CV. Opacification, contrast-to-noise ratio, signal-to-noise ratio, radiation dose, and CV for liver parenchyma and vessels in both groups were compared by paired *t* test and Pearson correlation. Receiver operating characteristic curve, visual grading characteristics, and Cohen κ were used.

Results: Contrast-to-noise ratio: compared with hepatic vein for functional liver, contrast-to-noise ratio was higher in group B (2.17 ± 0.83) than group A (1.82 ± 0.63); portal vein: higher in group B (2.281 ± 0.96) than group A (2.00 ± 0.66). Signal-to-noise ratio for functional liver was higher in group B (5.79 ± 1.58 Hounsfield units) than group A (4.81 ± 1.53 Hounsfield units). Radiation dose and contrast media were lower in group B (1.98 ± 0.92 mSv) (89.51 ± 15.49 mL) compared with group A (2.77 ± 1.03 mSv) (100 ± 1.00 mL). Receiver operating characteristic curve demonstrated increased reader in group B (95% confidence interval, 0.524–1.0) than group A (95% confidence interval, 0.545–1.0). Group B had increased revenue up to 58% compared with group A.

Conclusions: Image quality improvement is achieved with lower CV and radiation dose when using peristaltic injector with weight-based CV in HCT.

Key Words: computed tomography, contrast media, injector, liver

(*J Comput Assist Tomogr* 2020;44: 209–216)

Computed tomography (CT) is a prolific imaging tool that is key for the detection and diagnosis of liver parenchymal and vascular diseases.[1–4] The rapid increase in technological advances has enabled radiologists with submillimeter images with improved quality, while at the same time being cost-effective and easily accessible.[5,6] This increase has resulted in a significant increase in the application of CT in the treatment pathways of disease that has exploded to over 70 million examinations performed annually in the United States.[7] However, despite its beneficial application, an enormous concern of cancer risk has surged due to radiation dose and rates of iodinated contrast media (ICM) volumes.[1–3,8–10] Until recently, the chief focus of CT protocols has revolved around increased image quality and radiation dose reduction, but ICM delivery has been overlooked as a key component to both image quality and radiation dose reduction with different ICM volumes and injector systems.[11]

Iodinated contrast media delivery during CT ensures optimal parenchymal and vascular opacification with improved visualization and delineation of normal and abnormal anatomy when using power injectors.[12] However, ICM are administered to patients by automated injector systems, which aim to decrease ICM volume and improve image quality by providing consistent ICM delivery, which results in improved patient care.[13] Over the last decade, there has been a shift from hand to power injections, with several injector systems being available.[11] The types of power injectors include (*a*) electromechanical, (*b*) hydraulic piston (direct drive), and (*c*) peristaltic roller power injectors.[11] Nevertheless, ICM leads to variability in fluid delivery according to predetermined protocols and patient's current cardiovascular status.[13] The direct-drive contrast injector, also known as reciprocating pump, utilizes a drive motor that moves the piston plunger backward retracting ICM to fill the syringes and then moves forward to push it to patients.[12,13] The peristaltic drive contrast injector, also known as the rotary pumps, uses compression and relaxation of the tube drawing the contents into a delivery tube.[13] The peristaltic drive creates a seal between the suction and discharge side of the pump, eliminating product slip and reducing delivery pressure of the contrast media.[12,13]

The magnitude of liver parenchymal opacification depends on patient- and injection-related factors such as body weight, cardiac output, contrast media volume, contrast media concentration, injection rate, and saline chaser.[14,15] Optimal liver opacification during CT is affected by many contrast media techniques such as a single bolus[16] compared with split bolus,[17] which can be with or without a saline chaser.[18] In addition, the delivered contrast media volumes range from 80 to 150 mL,[17,18] with the overall liver parenchymal opacification of 112.4 ± 14.5 Hounsfield units (HU) when compared with different iodine concentrations during split-bolus injection protocol.[17] Also, studies have demonstrated that comparing different injection protocols resulted in variable liver parenchymal enhancement.[18] Saline has a pivotal role in the enhancement of the liver parenchyma with the lowest recorded enhancement of the liver of 71.5 ± 19.6 HU when a saline flush was injected at a rate of 2 mL/s postcontrast administration and the highest of 75.1 ± 27.5 HU when the saline flush was injected at 8 mL/s.[18] When no saline flush was administered after contrast

From the *Faculty of Health Sciences, Medical Imaging Sciences and †Diagnostic Radiology Department, American University of Beirut Medical Center, Beirut, Lebanon; and ‡Radiology Department, Campbelltown Hospital, Campbelltown; and §Radiology Department, Liverpool Hospital, Liverpool, New South Wales, Australia.

Received for publication October 7, 2019; accepted December 6, 2019.

Correspondence to: Lena Naffaa, MD, Diagnostic Radiology Department, American University of Beirut Medical Center, PO Box 11-0236 Riad El-Solh, Beirut 1107 2020, Lebanon (e-mail: ln01@aub.edu.lb).

The authors declare no conflict of interest.

Institutional review board approval was obtained. Informed consent was waived by the institutional review board, because this is a retrospective study.

DOI: 10.1097/RCT.0000000000000994

injection, the liver enhancement was 74.7 ± 23.1 HU.[18] Therefore, optimal liver parenchymal opacification varies significantly in literature, with limitations in the clinical setting due to contrast media injection parameters, patient selection, and scanner parameters during liver CT.

The aim of this study is to compare 2 contrast media protocols and injectors: direct drive with fixed contrast volume (CV) and peristaltic drive with weight-based contrast protocol with particular reference to vascular and parenchymal opacification of the liver, effect on qualitative and quantitative image quality, radiation dose, and contrast media volume. Value-based imaging is highlighted.

MATERIALS AND METHODS

Prior to 2016, direct-drive pump contrast media injector (Optivantage; Guerbet, Villepinte, France) system with fixed CV (Optiray 350 mg I/mL; Mallinckrodt, Griesheim, Germany), which is categorized into group A, was used at our university hospital. After 2016, the injector was substituted with a peristaltic contrast media injector (CT Motion; Ulrich, Ulm, Germany) that used weight-based CV protocol (Omnipaque 350 mg I/mL; GE Healthcare, GE Healthcare, Princeton, New Jersey), group B (Fig. 1).

Study Population

This retrospective study was approved by the institutional review board, and informed consent was waived. Data were collected from the Picture Archiving and Communication System between October 1, 2015, and February 1, 2017. These included data of 171 patients (aged ≥18 years) who underwent an abdominopelvic CT. Each patient underwent the 2 different injection protocols: group A used direct-drive injection method with fixed CV, and group B utilized the peristaltic injection method with contrast weight-based protocol.

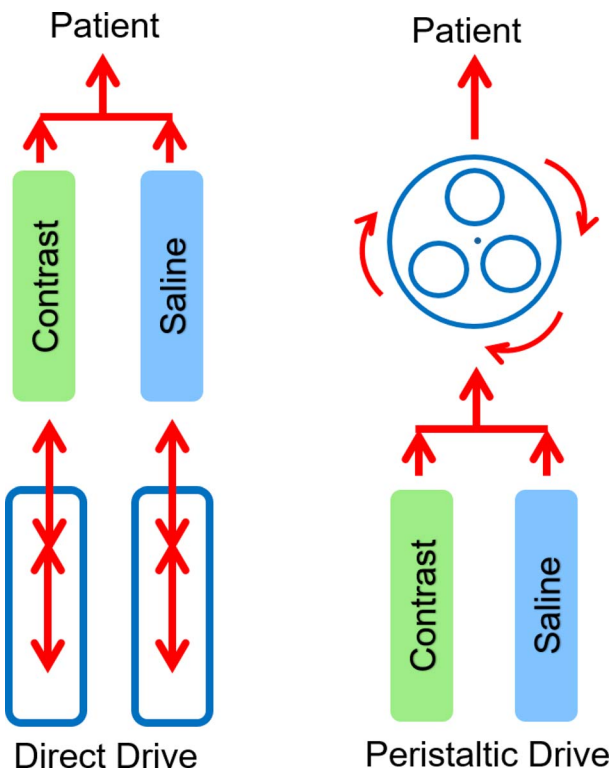

FIGURE 1. Left, direct-drive contrast media injectors. Right, Peristaltic drive contrast mechanism of action.

Liver CT Acquisition

Computed Tomography Scanning Protocol

Computed tomography was performed using a 256-channel CT scanner (Philips Brilliance iCT; Philips Healthcare, Best, the Netherlands). Both contrast media and injector groups used a tube voltage of 120 kVp, 180 mAs with *x*-, *y*-, and *z*-axis Ma modulation (DoseRight). The temporal resolution was 0.3 s/rot with beam collimation of 128 × 0.625 mm = 80 mm and a pitch value of 1.375 mm/rot.

Contrast Media Administration

The contrast media volume for each group was as follows: group A (direct drive): 100 mL of contrast (Optiray 350 mg I/mL; Mallinckrodt); group B (peristaltic drive): a weight-based group consisting of contrast (Omnipaque 350 mg I/mL; GE Healthcare). Weight-based groups used the following volumes: less than 75 kg (80 mL) and greater than 75 kg (100 mL). Both groups were intravenously injected at a flow rate of 3 mL/s with a 100 mL saline flush. Each acquisition had a 70-second post injection delay (venous phase) for all routine imaging.

Quantitative Image Assessment

Liver images were assessed in the venous phase of the abdominal CT. Mean venous and parenchymal measurements were automatically segmented according to Couinaud classification and measured using the liver software package (Philips Intellispace Portal, 7.0; Philips Healthcare). Each of the liver images underwent landmark identification: inferior vena cava, right portal bifurcation, right hepatic vein, mid hepatic vein, umbilical fissure, left portal bifurcation, tip of left liver, superior ligamentum venosum, deep ligamentum venosum, and superior deep ligament prior to automatically segmenting the hepatic vasculature and parenchyma (Fig. 2). Slice thickness of 3 mm was used for all liver examinations to measure the opacification profile of the hepatic and portal veins, liver parenchyma, contrast-to-noise ratio (CNR), and signal-to-noise ratio (SNR) for each hepatic segment (n = 8) and vessels. Both functional and total hepatic volumes were measured and compared.

Image Reconstruction

Transaxial images were all reconstructed with a model-based iterative reconstruction algorithm (iMR; Philips Healthcare). All images used iMR, level 2. Images were reconstructed using 3 × 3-mm slice thickness using a smoothing convolution kernel (field of view 380 × 380 mm, image matrix 512 × 512).

Parenchymal and Vessel Opacification and Noise

Quantitative image measurements used a region of interest (ROI) automatically specified after liver segmentation for liver. Each measurement recorded the opacification value in Hounsfield units, and its SD represented image noise (HU).

SNR Measurement

The SNR was calculated by measuring the mean liver parenchyma and hepatic and portal veins. (1): SNR = μA/σA, where μA is the mean ROI value for the parenchyma/veins, and σA is the SD of the mean ROI values for the parenchyma/veins.

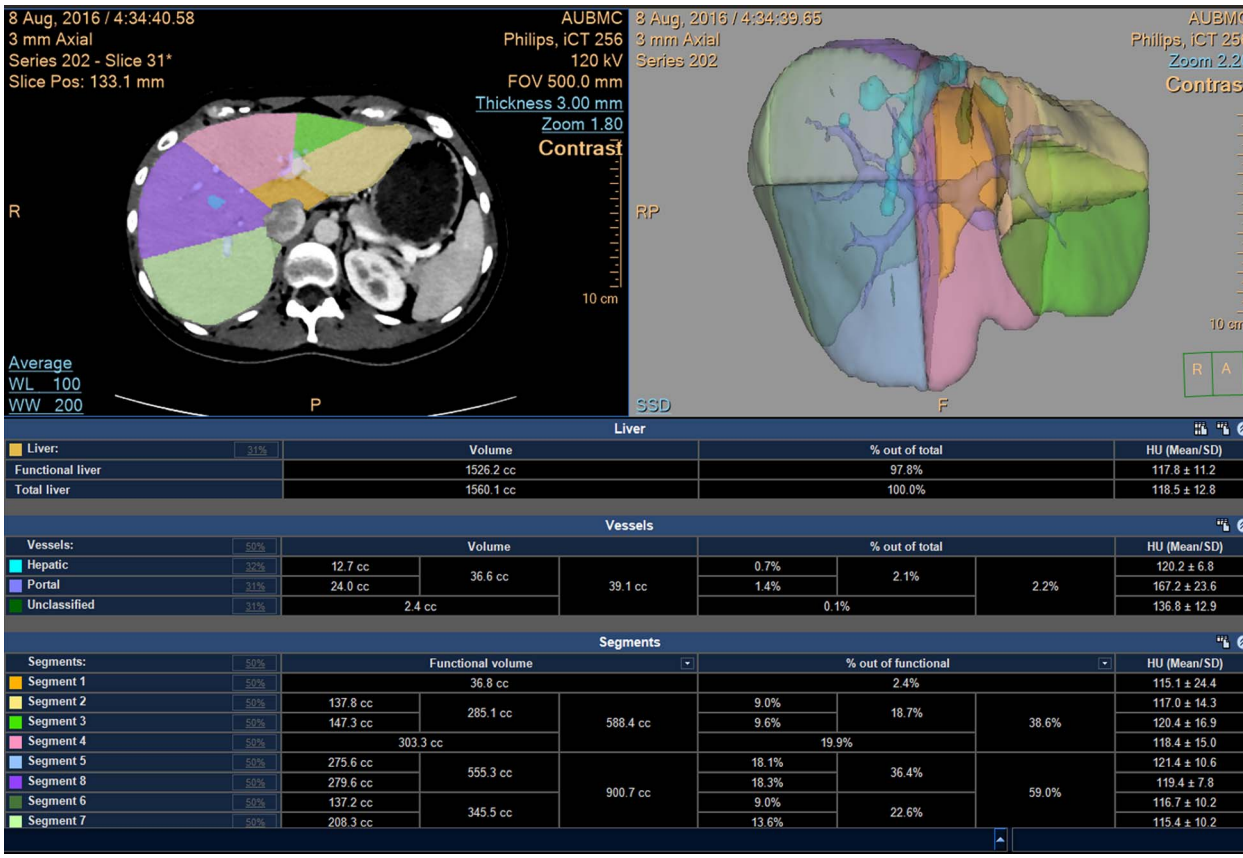

FIGURE 2. Automated liver segmentation using between functional and nonfunctional liver segment and their associated volumes and mean opacification. Figure 2 can be viewed online in color at www.jcat.org.

CNR Measurement

The CNR was calculated by measuring the mean liver parenchyma and hepatic and portal veins. (2): CNR = μA − μB/σA, where μA is the mean ROI for the parenchyma/veins, μB is the mean ROI value of the hepatic veins, and σA is the SD of the ROI values for the total parenchyma/veins.

TABLE 1. Liver Parenchyma and Vasculature Volume

	Group A	Group B	*P*
Liver vasculature volume			
Hepatic vein volume	26.90 ± 12.71	31.56 ± 15.03	0.002
Portal vein volume	22.58 ± 13.35	20.77 ± 12.16	0.190
Liver parenchymal volume			
Mean functional liver	1631 ± 468.66	1660 ± 534.15	0.599
Total functional liver	1680.47 ± 481.94	1713.32 ± 549.01	0.557
Liver segment			
1	45 ± 20.58	45.83 ± 21.08	0.713
2	186.26 ± 69.29	188.82 ± 80.47	0.755
3	119.59 ± 97.94	126.14 ± 95.34	0.531
4	272.31 ± 98.34	282.09 ± 110.27	0.387
5	311.11 ± 339.33	292.39 ± 125.83	0.499
6	173.21 ± 86.23	162.61 ± 109.28	0.320
7	243.07 ± 87.74	249.70 ± 91.30	0.494
8	302.12 ± 89.81	313.95 ± 114.29	0.288

Data are mean ± SD in volume (cm^3).

Radiation Dose Measurement

For each of the CT scans, individual effective dose (E_{ff} [mSv]) was calculated from the dose-length product (DLP [mGy × cm]), which was recorded from both patients groups. A normalized conversion factor (k [mSv/mGy × cm]) for the abdomen—0.015 mSv/mGy × cm—was used to calculate (3): E_{ff}[19]: $E_{ff} = DLP \times k$.

Qualitative Image Assessment

Qualitative image assessment untied a multireader analysis that consisted of 8 radiologists certified by the American Board of Radiology with a mean of 15.7 ± 4.2 years' reading experience. The image observer bank consisted of a total of 100 patients who were randomly selected from group A, with their corresponding images in group B (n = 200). The images were randomly arranged and blinded, with the contrast media injection and injector group not revealed to the observers. Readers assessed hepatic parenchyma, hepatic vein, and portal vein image quality and the visible presence of pathology. Readers were permitted to manipulate the window and level of the images. Each reader indicated the level of parenchymal and vessel image quality and the presence of pathology.

Receiver Operating Characteristic Analysis

Receiver operating characteristic (ROC) methodology was used to illustrate radiologist confidence intervals to detect pathology. A

TABLE 2. Mean Vascular Opacification (HU) of Liver Parenchyma and Vasculature

	Group A	Group B	*P*
Liver vasculature opacification			
Hepatic vein	129.98 ± 23.96	131.34 ± 21.51	0.581
Portal vein	133.24 ± 24.10	133.13 ± 23.16	0.966
Parenchymal opacification	93.33 ± 21.81	94.89 ± 18.90	0.479
Functional liver			
Total functional liver	94.44 ± 21.84	96.02 ± 18.86	0.475
Liver segment			
1	92.99 ± 19.26	91.87 ± 17.65	0.578
2	94.55 ± 20.52	95.01 ± 18.08	0.827
3	95.78 ± 21.77	97.45 ± 18.83	0.448
4	95.41 ± 21.93	96.91 ± 18.71	0.497
5	95.86 ± 22.60	97.77 ± 19.39	0.403
6	92.94 ± 22.45	94.80 ± 19.45	0.414
7	92.03 ± 22.36	94.19 ± 19.44	0.342
8	95.01 ± 22.79	96.57 ± 19.69	0.496

Data are mean ± SD in HU.

score of 1 to 2 was assigned to each image, where 1 indicates positive for pathology detection, and 2 indicates negative for pathology detection of liver lesions.

Visual Grading Characteristic Analysis

Visual grading characteristic (VCG) method was used to illustrate the radiologist's preference of one injector/contrast media protocol group over another based on qualitatively assessing image quality. A score of 1 to 5 was assigned, where 1 indicates poor image quality, and 5 indicates optimal image quality for each of the anatomical structures: liver parenchyma and hepatic and portal veins.

Interreader and Intrareader Variability

In each group, the interobserver and intraobserver agreements were calculated using Cohen κ analysis. A *k* value 0.60 to 1, 0.41 to 0.60, 0.21 to 0.40, and less than 0.20 was considered excellent, moderate, fair, and poor agreement, respectively.

Cost-effective Analysis

The mean contrast, contrast and saline volume, and injector accessories used to perform each contrast group were recorded. Workflow and waste analysis were carried out for each of the radiographer's time, as well as garbage waste volume and cost, respectively. Total monitory value was extrapolated from the patient data to determine savings in time and cost.

Statistical Analysis

All data analyses were conducted using SPSS version 24 for Windows (SPSS Inc, Chicago, Ill). Opacification, volume, radiation dose, and contrast media volume measurements were compared using paired *t* test and Pearson correlation. Results were considered statistically significant if $P \leq 0.05$. Categorical variables are presented as frequencies with percentages, and continuous variables are presented as means ± SDs. Receiver operating characteristics and VCGs were used to measure the confidence intervals in pathology detection and image quality, respectively. Interobserver and intraobserver variations were investigated using Cohen κ methodology.

RESULTS

Patient Demographics

All patients were white. There was no significant difference in gender (46.2% were females and 53.8% were males in each group) and age (mean ages, 54.98 ± 15.97 and 56.27 ± 15.67 years, respectively) between groups A and B ($P > 0.05$). The duration between each contrast media protocol/injector for all patients was 1.29 ± 0.30 years, which was the time interval between the first and second scans during each patient imaging pathway.

Quantitative Analysis

Contrast, Parenchymal, and Vessel Volume and Opacification

Statistical analysis demonstrated significantly higher use in contrast media volume in group A (100 ± 1 mL) compared with group B (89.51 ± 15.49 mL) ($P < 0.0001$). A significant difference was also observed in hepatic and portal vein volumes between group A (26.90 ± 12.71 and 22.58 ± 13.35 cm^3) and group B (31.56 ± 15.03 and 20.77 ± 12.16 cm^3) ($P < 0.05$), respectively. No difference was noted in the total and segmented liver parenchyma between both groups ($P > 0.05$) (Table 1). There was no significant difference in parenchymal and vascular opacifications between both groups ($P > 0.05$) (Table 2).

Signal-to-Noise Ratio

There was a significant difference in SNR between both groups ($P < 0.0001$), with group B being superior to group A in the functional, total, and individual segments of the liver (Table 3), except in segment 4, where no significant difference was noted ($P = 0.051$).

Contrast-to-Noise Ratio

Comparing the liver and hepatic vein opacifications, the mean CNR in group B was significantly higher than that of group A in the functional and individual segments of the liver ($P < 0.0001$), except in segment 4, where no difference is noted ($P = 0.190$). However, no difference was seen in the total liver CNR between each group ($P = 0.15$) (Table 4).

When comparing the CNR between liver and portal vein opacifications in the functional liver and total liver, a significant difference was noted between the 2 groups. Functional liver volume in group A (2.00 ± 0.66) was significantly lower than that

TABLE 3. SNR of the Functional and Total Liver Parenchymal Opacification

	Group A	Group B	*P*
Functional liver	4.81 ± 1.53	5.79 ± 1.58	<0.0001
Total liver	4.56 ± 1.43	5.35 ± 1.52	<0.0001
Liver segment			
1	3.38 ± 1.09	3.70 ± 1.17	0.008
2	4.03 ± 1.28	4.62 ± 1.36	<0.0001
3	4.38 ± 1.56	5.14 ± 1.77	<0.0001
4	4.40 ± 2.62	4.87 ± 1.71	0.054
5	5.31 ± 1.97	6.43 ± 2.09	<0.0001
6	5.46 ± 1.93	6.82 ± 1.90	<0.0001
7	5.29 ± 1.76	6.80 ± 2.09	<0.0001
8	5.61 ± 1.99	7.19 ± 2.47	<0.0001

Data are mean ± SD in HU.

TABLE 4. CNR Of the Hepatic and Portal Vein in Each Liver Segment

	Group A	Group B	*P*
Hepatic vein			
Functional liver	1.82 ± 0.63	2.17 ± 0.83	<0.0001
Total liver	1.63 ± 0.50	1.88 ± 0.65	0.15
Liver segment			
1	1.31 ± 0.49	1.55 ± 0.61	<0.0001
2	1.44 ± 0.52	1.66 ± 0.60	<0.0001
3	1.50 ± 0.60	1.69 ± 0.67	0.008
4	1.53 ± 0.99	1.65 ± 0.64	0.190
5	1.77 ± 0.64	2.10 ± 0.78	<0.0001
6	2.08 ± 0.78	2.56 ± 1.02	<0.0001
7	2.09 ± 0.72	2.55 ± 0.91	<0.0001
8	1.94 ± 0.60	2.37 ± 0.81	<0.0001
Portal vein			
Functional liver	2.00 ± 0.66	2.28 ± 0.96	0.001
Total liver	1.80 ± 0.53	1.99 ± 0.81	0.011
Liver segment			
1	1.43 ± 0.45	1.62 ± 0.68	0.002
2	1.63 ± 0.55	1.82 ± 0.84	0.001
3	1.65 ± 0.58	1.80 ± 0.81	0.050
4	1.68 ± 0.98	1.75 ± 0.78	0.494
5	1.95 ± 0.64	2.21 ± 0.92	0.003
6	2.28 ± 0.81	2.69 ± 1.13	<0.0001
7	2.28 ± 080	2.71 ± 1.20	<0.0001
8	2.14 ± 0.68	2.52 ± 1.01	<0.0001

Data are mean ± SD in HU.

in group B (2.28 ± 0.96) ($P = 0.001$), whereas the total liver CNR was higher in group B (1.99 ± 0.81) compared with group A (1.80 ± 0.53 HU) ($P = 0.011$). In addition, group B was significantly superior over group A when comparing the CNR in the individual segments of the liver ($P < 0.05$), except segment 4 ($P = 0.494$) (Table 4).

Radiation Dose

The radiation dose (in mSv) delivered to the liver was significantly less in group B (1.98 ± 0.92) compared with group A (2.77 ± 1.03) ($P < 0.0001$). Interestingly, patient habitus did not significantly change between both groups.

Qualitative Image Evaluation

Receiver Operating Characteristic

Detection of liver lesions demonstrated a significant difference ($P < 0.0001$) between positive and negative for pathology in both groups. Group B (0.750–0.944) demonstrated an increase in radiologist confidence (area under the curve [AUC]) in detecting pathology compared with group A (0.718–0.983) (Fig. 3).

Visual Grading Characteristic

The 5-point scores were individually graded by 8 radiologists for each group. The results were represented as graphs shown in Figure 3. When a preference is shown toward 1 group, the curve is convex to that group's axis. The graphs clearly demonstrate that there was no statistical significance between liver parenchyma and hepatic vein opacification; however, marginal preference was for group B over group A (Figs. 3B and 4A), with AUC increasing from 0.487 to 0.729 and 0.394 to 0.85, respectively. In contrary, when the portal vein opacification was assessed for image quality, no preference was observed between groups, with the AUC increasing from 0.450 to 0.545 (Fig. 4C).

Cohen κ Analysis

Interreader and intrareader agreement was higher in group B (κ = 0.39–0.91) compared with group A (κ = 0.25–0.76), with former demonstrating excellent agreement. There was a strong positive relationship between liver vasculature and parenchymal opacifications, image quality, and reader confidence in group B compared with group A ($r = 0.693$, $P < 0.001$).

Workflow and Cost Analysis

Contrast Media Volume, Saline Volume, Garbage, and Accessories Expenses

The average cost (in US $) per patient contrast media, saline, and accessories were compared between both groups, where group B ($18.67/patient) has significantly lower expenses than group A ($46.28/patient) ($P = 0.001$). Therefore, cost reduction for each patient undergoing group B was $27.61, with the total savings across 182 patients being $5025.02. Garbage waste analysis demonstrated a reduction in consumables being disposed in group B compared with group A, with a total reduction of 90 bags

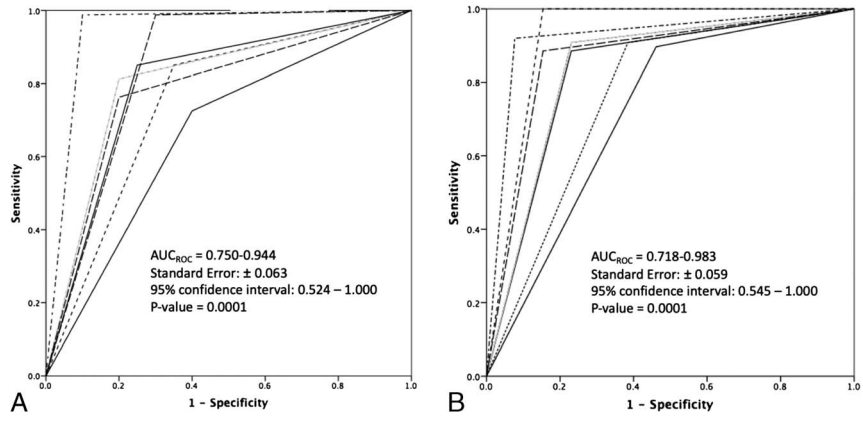

FIGURE 3. Receiver operating characteristic curve analysis for pathology detection in (A) group A and (B) group B.

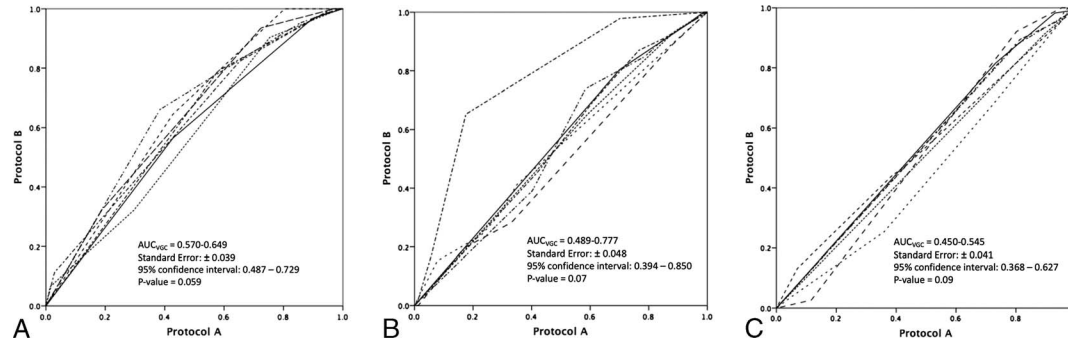

FIGURE 4. Visual grading characteristic curve analysis for image quality in (A) liver parenchymal opacification, (B) hepatic vein opacification, and (C) portal vein opacification.

in group B. Each bag costs US $2 for purchasing and disposing with a total reduction in cost due to waste estimated at US $180.

Time Analysis

The total time (in minutes) taken for the radiographer to prepare the contrast media injector and filling of contrast media for each patient was significantly reduced in group B (1.21) compared with group A (5). This is consistent with a significant difference between group A (910 minutes) and group B (220.22 minutes) in the total time needed for 171 patients ($P = 0.001$). As a result, a total of 689.79 minutes was saved in group B. Because the cost of radiographers was US $0.21/min and based on US $2000 monthly salary estimation, US $144.85 of the cost was saved for this study.

Comprehensive Cost Analysis

The overall workflow and cost analysis demonstrated a significant saving of US $5252.87 for the 171 patients who underwent group B. This cost saving increased revenue to the institution without sacrificing image quality, radiation dose, or pathology detection. Using a peristaltic pump can provide radiology departments with a value-based approach to imaging without sacrificing patient outcomes. Finally, each contrast media injector is equal in value and does not offer any cost savings between the two.

DISCUSSION

In the current study, we quantitatively and qualitatively compared hepatic parenchyma and vascular opacification between 2 contrast media injection protocols and injectors. We used different quantitative methodologies to support our hypothesis, in which we considered opacification levels, CNR, and SNR within the liver parenchyma and vasculature. Moreover, a qualitative assessment was used using VCGs, ROC, and κ analysis. The results demonstrated that both injection protocols and injectors demonstrated no difference in parenchyma and vascular opacification. However, it was shown that group B had increased quantitative image quality (Fig. 5), pathology detection, and cost saving with lower radiation dose and CV compared with group A.

Lesion detection during liver CT is dependent on the parenchymal morphology, texture, and perfusion of contrast media. Lesion density increases with high attenuation values relative to the surrounding liver parenchyma, which results from iodine density and not from soft tissue contrast. Recent studies[18,20–23] demonstrated that liver opacification values range from 72 to 112 HU.[17,18] In our study, we demonstrated that there was no significant difference in total liver, functional, or segmental parenchymal opacification between each contrast media injection protocol and injector with mean opacification from 93 to 96 HU. Quantitative image quality, such as CNR and SNR, was significantly higher in group B than in group A, and qualitative image quality measurements demonstrated no significant difference. Furthermore, reader confidence (ROC) was significantly increased in group B compared with group A in the detection of liver pathology. As such, increasing reader confidence in pathology detection is confirmed with increased signal and contrast relative to low noise in the liver parenchyma when using protocol B.

Contrast media agents play an important role in CT[15,24–31]: they increase both vascular and parenchymal enhancement by improving lesion conspicuity and image quality. However, increase in contrast media volumes has resulted in the potential effect of

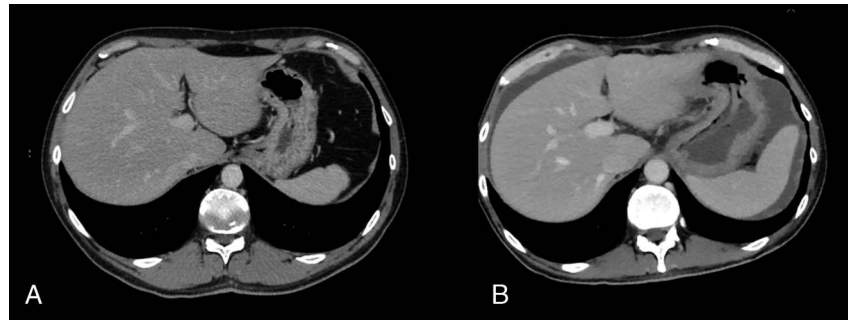

FIGURE 5. Images (A, B) demonstrate a 45-year-old man who underwent both group A and group B injections with a 2-year interval between scans.

increasing the risk of cancer due to double-strand DNA breaks by increasing organ dose by up to 71% when compared with unenhanced CT.[32,33] As such, the amount of radiation dose delivered should be minimized without affecting image quality and diagnosis.[30,34] In our study, we achieved a reduction in contrast media volume and radiation dose while using a peristaltic drive contrast injection with weight-based contrast media protocol. This could be due to the fact that reduced CV in group B compared with group A has resulted in this radiation dose difference. This dose reduction offers significant benefits to patients, by reducing both contrast media volume and radiation dose to patients by 1.4 times compared with protocol A (direct-drive injector with 100 mL of contrast) because of uniformly distributing the contrast media throughout the liver parenchyma. Even though there was no change in liver volumes between the first and subsequent CT scans, contrast media distribution throughout the liver is attained by reducing the injected cross-sectional area of the contrast entering the cardiovascular system during peristaltic injection.

There were shortcomings in our study; first, this study is a retrospective study. Second, the use of fixed versus weight-based contrast media volume with 2 injectors was not equal among both groups. Third, different ICM types with same concentrations were used between both groups. Fourth, the increased detection of pathology in group B compared with group A can be related to the fact that the images of each group were taken on an average of 1 year after being imaged. Hence, there might be enough time for disease progression and worsening resulting in better visualization of pathology. Fifth, we did not calculate the size-specific dose estimates for the liver between each patient, which would highlight the true effect of radiation dose and not measuring the level of DNA strand breaks in the short- and long-term follow-up of these patients. Finally, we did not measure the lesion to parenchymal enhancement ratio for liver lesions in the image perception study, which could have demonstrated the level of background enhancement relative to lesion detection.

In summary, our study demonstrated significant improvements in quantitative image quality of the liver with lower contrast media volume, radiation dose, and cost when using peristaltic contrast media injection with weight-based contrast protocol during abdominopelvic CT.

REFERENCES

1. Brenner DJ, Hall EJ. Computed tomography—an increasing source of radiation exposure. *N Engl J Med*. 2007;357:2277–2284.
2. Berrington de González A, Mahesh M, Kim KP, et al. Projected cancer risks from computed tomographic scans performed in the United States in 2007. *Arch Intern Med*. 2009;169:2071–2077.
3. Smith-Bindman R, Lipson J, Marcus R, et al. Radiation dose associated with common computed tomography examinations and the associated lifetime attributable risk of cancer. *Arch Intern Med*. 2009;169:2078–2086.
4. Ginat DT, Gupta R. Advances in computed tomography imaging technology. *Annu Rev Biomed Eng*. 2014;16:431–453.
5. Koyama T, Zamami Y, Ohshima A, et al. Patterns of CT use in Japan, 2014: a nationwide cross-sectional study. *Eur J Radiol*. 2017;97:96–100.
6. Aschoff AJ, Catalano C, Kirchin MA, et al. Low radiation dose in computed tomography: the role of iodine. *Br J Radiol*. 2017;90:20170079.
7. Bosch de Basea M, Salotti JA, Pearce MS, et al. Trends and patterns in the use of computed tomography in children and young adults in Catalonia—results from the EPI-CT study. *Pediatr Radiol*. 2016;46:119–129.
8. Brenner DJ, Elliston CD. Estimated radiation risks potentially associated with full-body CT screening. *Radiology*. 2004;232:735–738.
9. Mettler FA Jr, et al. Medical radiation exposure in the US in 2006: preliminary results. *Health Phys*. 2008;95:502–507.
10. Piechowiak EI, Peter JF, Kleb B, et al. Intravenous iodinated contrast agents amplify DNA radiation damage at CT. *Radiology*. 2015;275:692–697.
11. Friebe M. Computed tomography and magnetic resonance imaging contrast media injectors: technical feature review—what is really needed? *Med Devices (Auckland, NZ)*. 2016;9:231.
12. Indrajit IK, Sivasankar R, Pant R, et al. Pressure injectors for radiologists: a review and what is new. *Indian J Radiol Imaging*. 2015;25:210.
13. Chaya A, Jost G, Endrikat J. Piston-based vs peristaltic pump-based CT injector systems. *Radiol Technol*. 2019;90:344–352.
14. Saade C, Bourne R, Wilkinson M, et al. Contrast medium administration and parameters affecting bolus geometry in multidetector computed tomography angiography: an overview. *J Med Imaging Radiat Sci*. 2011;42:113–117.
15. Saade C, Deeb IA, Mohamad M, et al. Contrast medium administration and image acquisition parameters in renal CT angiography: what radiologists need to know. *Diagn Interv Radiol*. 2016;22:116–124.
16. Bae KT, Heiken JP, Brink JA. Aortic and hepatic peak enhancement at CT: effect of contrast medium injection rate—pharmacokinetic analysis and experimental porcine model. *Radiology*. 1998;206:455–464.
17. Scialpi M, Pierotti L, Gravante S, et al. Split-bolus multidetector-row computed tomography technique for characterization of focal liver lesions in oncologic patients. *Iran J Radiol*. 2016;13:e20143.
18. Marin D, Nelson RC, Guerrisi A, et al. 64-Section multidetector CT of the upper abdomen: optimization of a saline chaser injection protocol for improved vascular and parenchymal contrast enhancement. *Eur Radiol*. 2011;21:1938–1947.
19. Huda W, Ogden KM, Khorasani MR. Converting dose-length product to effective dose at CT. *Radiology*. 2008;248:995–1003.
20. Husarik DB, Gordic S, Desbiolles L, et al. Advanced virtual monoenergetic computed tomography of hyperattenuating and hypoattenuating liver lesions: ex-vivo and patient experience in various body sizes. *Invest Radiol*. 2015;50:695–702.
21. Wu D, Tan M, Zhou M, et al. Liver computed tomographic perfusion in the assessment of microvascular invasion in patients with small hepatocellular carcinoma. *Invest Radiol*. 2015;50:188–194.
22. Park SH, Kim PN, Kim KW, et al. Macrovesicular hepatic steatosis in living liver donors: use of CT for quantitative and qualitative assessment. *Radiology*. 2006;239:105–112.
23. Mokrane FZ, Dercle L, Meyrignac O, et al. Towards multi-phase postmortem CT angiography in children: a study on a porcine model. *Int J Leg Med*. 2018;132:1391–1403.
24. Saade CCL, Sugrue G, Murphy S. Understanding the inferior epigastric vessels—a potential key to preventing haematoma related acs. *Acta Clin Belg*. 2009;64:266.
25. Saade C, Mohamad M, Kerek R, et al. Augmented quadruple-phase contrast media administration and triphasic scan protocol increases image quality at reduced radiation dose during computed tomography urography. *J Comput Assist Tomogr*. 2018;42:216–221.
26. Saade C, Mayat A, El-Merhi F. Exponentially decelerated contrast media injection rate combined with a novel patient-specific contrast formula reduces contrast volume administration and radiation dose during computed tomography pulmonary angiography. *J Comput Assist Tomogr*. 2016;40:370–374.
27. Saade C, El-Merhi F, Mayat A, et al. Comparison of standard and quadruple-phase contrast material injection for artifacts, image quality, and radiation dose in the evaluation of head and neck cancer metastases. *Radiology*. 2016;279:571–577.

28. Saade C, El-Merhi F, El-Achkar B, et al. 256 slice multi-detector computed tomography thoracic aorta computed tomography angiography: improved luminal opacification using a patient-specific contrast protocol and caudocranial scan acquisition. *J Comput Assist Tomogr*. 2016;40:964–970.

29. Zein-El-Dine S, Bou Akl I, Mohamad M, et al. Split-bolus contrast injection protocol enhances the visualization of the thoracic vasculature and reduced radiation dose during chest CT. *Br J Radiol*. 2018;91:20180509.

30. Saade C, Ammous A, Abi-Ghanem AS, et al. Body weight–based protocols during whole body FDG PET/CT significantly reduces radiation dose without compromising image quality:findings in a large cohort study. *Acad Radiol*. 2019;26:658–663.

31. Saade C, Al-Fout G, Mayat A, et al. Increased image quality and reduced radiation dose and contrast media volume: a holistic approach to intracranial CTA. *Clin Radiol*. 2017;72:797.e11–797.e16.

32. Harbron R, Ainsbury EA, Bouffler SD, et al. Enhanced radiation dose and DNA damage associated with iodinated contrast media in diagnostic x-ray imaging. *Br J Radiol*. 2017;90:20170028.

33. Boone JM, Hernandez AM. The effect of iodine-based contrast material on radiation dose at CT: it's complicated. *Radiology*. 2017;283:624–627.

34. Mathews JD, Forsythe AV, Brady Z, et al. Cancer risk in 680 000 people exposed to computed tomography scans in childhood or adolescence: data linkage study of 11 million Australians. *BMJ*. 2013;346:f2360.